

Moth-Flame Optimization Cascade PI-Fractional Order PID Controller for price based Automatic Generation Control of a deregulated power system with HES and UPFC units

M.Poonkodi¹ and I.A. Chidambaram²

¹ Lecturer, Department of EEE, Government Polytechnic College, Perundurai, Erode,
Tamilnadu, India

² Professor, Department of Electrical Engineering, Annamalai University, Annamalainagar,
Tamilnadu, India

ABSTRACT

A new control plot is presented in this research article related with cost based cost Automatic Generation Control (AGC) conspire for a two-area thermal deregulated power system to limit the unscheduled exchange (UI) cost through invalidating the deviations in recurrence and to maintain the generation at various elements parsimoniously following a disturbance. Unscheduled Interchange price is unique among the segments Availability Based Tariff (ABT), which acts as a secondary control procedure for adapting the grid frequency. A advanced cascade Proportional-Integral along with Fractional Order Proportional-Integral-Derivative (PI-FOPID) controller have been utilized in AGC loop in order to improve their performance system. The significant advantage of PI-FOPID controllers is highly suitable for controlling purpose which helps to design the AGC problems and excellent capability of handling parameter uncertainty, elimination of steady-state errors and ensures better stability. The tuning of the PI-FOPID controller parameters is formulated as an optimization problem and solved by utilizing a Moth-Flame Optimization (MFO) algorithm. Further to improve the AGC execution, energy storage devices such as Hydrogen Energy Storage (HES) units connected in the control area and FACTS devices like Unified Power Flow Controller (UPFC) also introduced in continuous sequence with tie-line of the interconnected areas. The usage of the HES-UPFC devices, captures the underlying fall in frequency as well as the tie

line power deviations after a sudden load disturbance and the outcomes demonstrate that the UI price are significantly limited by keeping up frequency at normal value. Besides, the proposed technique yields an eminent decrease in unscheduled interchange price signal. As a result, the market participants can get profit accordingly.

Keywords: Availability Based Tariff, Hydrogen Energy Storage, Moth-Flame Optimization (MFO) algorithm, Unified Power Flow Controller and Unscheduled Interchange prices.

1. Introduction

Present day power system regularly comprises of various subsystems interconnected through tie-lines. For every subsystem the necessities ordinarily incorporate coordinating framework age to framework burden and managing framework recurrence is fundamentally known as Automatic Generation Control (AGC) issue [1]. It is alluring to accomplish a superior recurrence steadiness by speed administering framework alone as well as by receiving different advanced current utilities. If there should be an occurrence of an interconnected force framework, any little unexpected burden change in any of the territories causes the vacillation of the frequencies of every single zone and furthermore there is variance of intensity in tie line. In deregulated power framework comprises of producing organizations (Gencos), conveyance organizations (Discos), transmission organizations (Transco) and framework administrator (SO). In such an open market economic situation, SO keeps up the straightforwardness of exchanges satisfying the requests among the Gencos and Discos. The essential goal of the SO is permitting the contracted capacity to spill out of Genco to Disco. To move the contracted force at adequate degree of value and unwavering quality certain subordinate administrations are required by the System Operator. So the conventional AGC two-zone interconnected force framework is changed by assessing the respective agreement's impact on the elements [2]. In view of the reciprocal exchanges, a conveyance organization

(Disco) has the opportunity to contract with any accessible age organization (Genco) in its own or another control zone. With the advancement of the Disco Participation Matrix (DPM) the representation of agreements can be made simpler. DPM is spoken to as a hilter kilter grid developed by the quantity of lines equivalent to the quantity of Gencos and the quantity of sections equivalent to the quantity of Discos in the framework. Each element in the matrix is referred to a segment of a total load contracted by a Disco (Column) toward a Genco (Row). The sum of all the entries in a column of this matrix is unity. DPM proves the participation of a Disco in a contract with Genco.

Frequency linked real time pricing scheme is other approach of AGC loop in restructured electricity market. Researchers have presented the Frequency linked price based control service in deregulated electricity market [3]. The ABT methodology has been acquainted basically with guarantee framework security and manage matrix indiscipline winning in the framework before its presentation. In the ABT regime, the objective of the generation controllers is that they have to nullify the deviations in supply frequency and also schedule the generators according to their merit so as to economize the system operation. Hence, conventional AGC is to be modified so that the UI price signal and the marginal cost may be incorporated into the system to meet the AGC loop objectives. The primary loop of this model is similar to conventional AGC, responds to changes in frequency whereas the secondary loop, called ABT control loop is different from conventional AGC. The frequency is converted to UI price signal and is compared with marginal cost of the generator to generate an error signal called Generation Control Error (GCE). The GCE when amplified, forces the reference power setting to control the generation thereby reduces frequency deviations [4].

Several advanced controller structures and techniques have been projected in the collected survey works for AGC [5]. Among the choice of secondary controllers, the most commonly

employed is the conventional Integer order (IO) controller such as Proportional plus Integral (PI) controllers, Proportional plus Integral plus Derivative (PID). The fundamental downside of the PI controller is doesn't capable to predict the future errors of the system, can't eliminate steady-state oscillations and reduces settling time. Consequently, the overall stability system is relatively low [6]. The fundamental points of the Proportional plus Integral plus Derivative (PID) controller, a derivative mode improves the strength of the framework and encourages to increment in corresponding increase and diminishes in a necessary addition which hence extends the speed of the controller reaction. At the point when the info signal has sharp corners, the subsidiary term will convey irrational size control contributions to the plant. Additionally, any noise in the input signal will bring about enormous plant input signals that lead to confusion in pragmatic applications [7].

The performance of these controllers can be improved by utilizing fractional analytics. In Fractional Order (FO) controllers, the order for integral and derivative terms isn't a number. The principle preferred position related to FO controllers is adaptability in controlling reason which plans a robust control system. FO controllers have the outstanding capability of handling parameter vulnerability, disposal of steady-state error and better stability [8]. The significant advantage of the Fractional Order Proportional-Integral-Derivative (FOPID) controller provides flexibility in controlling purpose which helps to plan the AGC problems and excellent competence of handling parameter uncertainty, elimination of steady-state error and ensures better stability. However, this flexibility enables the tuning of the controller even in complex situations [9]. Therefore, the task of designing the FOPID controller is more challenge and the insignificant property is not exclusively executed by the controller structure. Be that as it may, the shut circle reference model the controller is fundamentally partial and has a interesting structure for its usage. Without a doubt, the controller can frequently be disintegrated into two sections. A number request controller fell with a

fragmentary request controller and guaranteed that the controller plan strategy is easy to execute. The significant advantage of PI-FOPID controllers is highly suitable for controlling purpose which helps to design the AGC problems and excellent capability of handling parameter uncertainty, elimination of steady-state errors and ensures better stability. The control parameters of the PI-FOPID controller are tuned using the Moth-Flame Optimization (MFO) algorithm [10] and result from its execution is compared with that of the FOPID controller-based AGC system.

The coordinated control actions between Energy Storage device and FACTS devices in the AGC system has been found that the capacity of regulating the snare conditions in a very wanton and economical manner [9,13]. In this study, the improvement of the AGC system a refined use of energy storage devices such as the Hydrogen Energy Storage (HES) units connected in the control area and a Unified Power Flow Controller (UPFC) can be introduced in continuous sequence with tie-line of the anticipated power system. In this study the coordination of AGC with HES and UPFC units are performed and it reveals that power system stability can be improved. Furthermore, the proposed method yields a notable reduction in unscheduled interchange price signal. As a result, the market participants can get profit accordingly.

2. Price signal based Automatic Generation Control (AGC) scheme

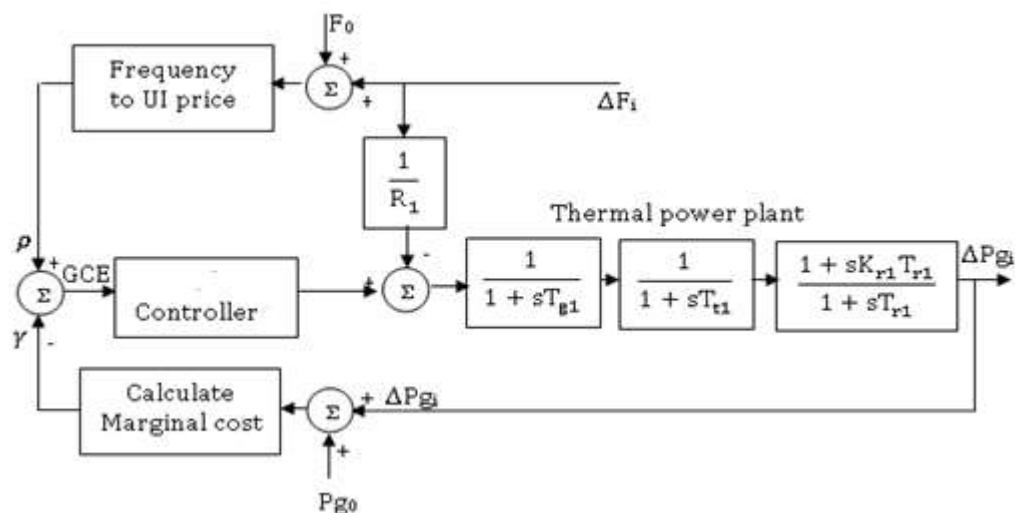


Fig 1 Block diagram of Price signal based Automatic Generation Control

The basic principle of the Price based AGC loop is illustrated in Fig 1. Each generator individually monitors the UI price ρ and compares with its marginal cost γ . It derives an error signal, which is the difference of current UI price and its own marginal cost. This error signal, which can be termed as Generation Control Error (GCE), is fed to an integral controller. A positive GCE shows that the generator will benefit by expanding age level. A negative GCE demonstrates that Generator will benefit by diminishing the age level. Thus, GCE assumes an indispensable job in controlling the power generation [4]. In this proposed control scheme, the GCE is redefined as

$$GCE = UI \text{ price } (\rho) - \text{marginal cost } (\gamma) \quad (1)$$

2.1 Frequency to Unscheduled Interchange (UI) charge calculation

For the simulation model, CERC 2014 regulation has been considered [4]. The frequency to Unscheduled Interchange (UI) charge calculation for the year 2014 has been shown in Fig 2.

```
function p = fcn(F)
if F<=49.7
p=8240.4;
elseif F<=50;
p=1780+20840*(50-F);
elseif F<=50.05
p=35600*(50.05-F);
else
p=0;
end
```

Fig 2 Frequency to Unscheduled Interchange (UI) charge block

2.2 Marginal Cost Calculation

The fuel cost characteristics of generators in ₹/h is given by

$$C_i(P_{gi}) = a_i + b_i P_{gi} + c_i P_{gi}^2 \quad (2)$$

where a_i , b_i , c_i are the cost coefficients which are constant for a given generator.

The marginal cost of i th generator in ₹/MWh is given by

$$(Marginal\ cost)_i = b_i + 2c_i P_{gi} \tag{3}$$

The actual marginal cost of each generator is calculated using Eq (3) by taking $P_{gi} = P_{gi0} + \Delta P_{gi}$ where P_{gi0} is the generation at i^{th} generator before the disturbance and ΔP_{gi} is the change in generation due to generation control mechanism. The reference marginal cost of individual generator is calculated using Eq (3) by substituting the desired P_{gi} values. Following a change in load, the desired P_{gi} values may be obtained by running the economic dispatch program or by allocating the change in load to generators randomly with the experience of the system operator.

3. Mathematical model of Hydrogen Energy Storage (HES) and Unified Power Flow Controller (UPFC) units

3.1 Mathematical Modeling of Hydrogen Energy Storage

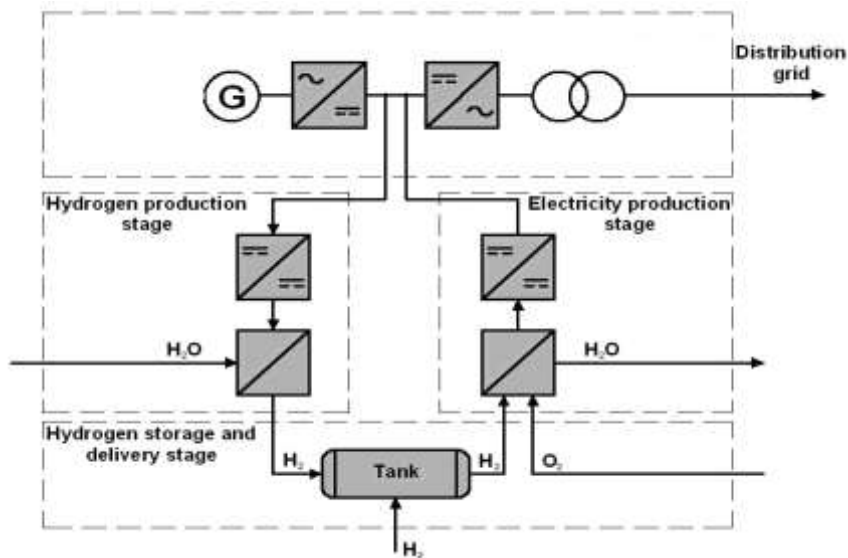


Fig. 3 Block diagram of the Hydrogen Energy Storage unit

In Fig 5.4 shows the block diagram of the hydrogen storage unit with Fuel cells. The transfer task of the Aqua Electrolyzer can be articulated as first order lag:[12]

$$G_{AE}(s) = \frac{K_{AE}}{1+sT_{AE}} \tag{4}$$

The transfer function of Fuel Cell (FC) can be given by a simple linear equation as

$$G_{FC}(s) = \frac{K_{FC}}{1+sT_{FC}} \tag{5}$$

The overall transfer function of HES unit has can be

$$G_{HES}(s) = \frac{K_{HES}}{1+sT_{HES}} = \frac{K_{AE}}{1+sT_{AE}} * \frac{K_{FC}}{1+sT_{FC}} \tag{6}$$

3.2 Mathematical Modeling of Unified Power Flow Controller

UPFC is using to regulate the power flow in the transmission frameworks by controlling the impedance, voltage magnitude & phase angle [14]. This controller offers central focuses in esteems to the static and dynamic activity of the power system. In the UPFC setup appeared in Fig.4 had two voltage source converters, where one converter is related in parallel to the transmission line while the other is in continuous sequence with the transmission line. The two converters are associated consecutive with a typical DC link capacitor. This course of action has three significant functions namely series, shunt, and phase angle regulation to be bound together in a similar circuit. The key capacity of the shunt converter is to ingest or create dynamic force from the line like that of a shunt compensator. The shunt converter can charge the DC connect capacitor and fulfill the force solicitation of the game plan converter through the DC interface capacitor. Thusly, the shunt branch is required to make up for any dynamic force drawn/gave by the arrangement branch and the misfortunes.

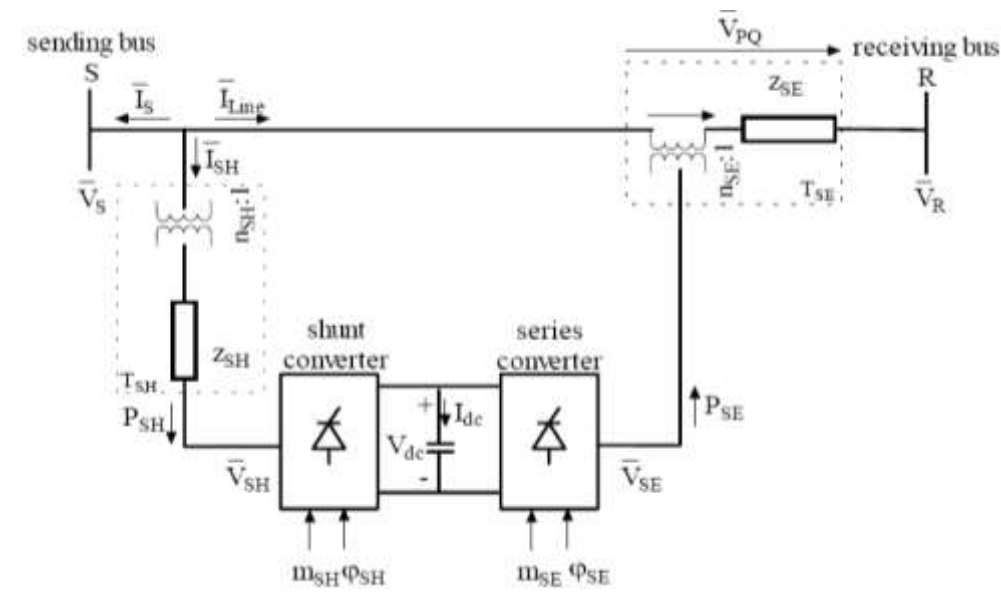


Fig. 4 Unified Power Flow Controller configuration

UPFC is set in the transmission line between buses S and R as appeared in Fig 5. Line conductance was ignored. UPFC unit is represented by two ideal voltage sources of controllable magnitude and phase angle. In this case, the complex power received at the receiving end of the line is given by

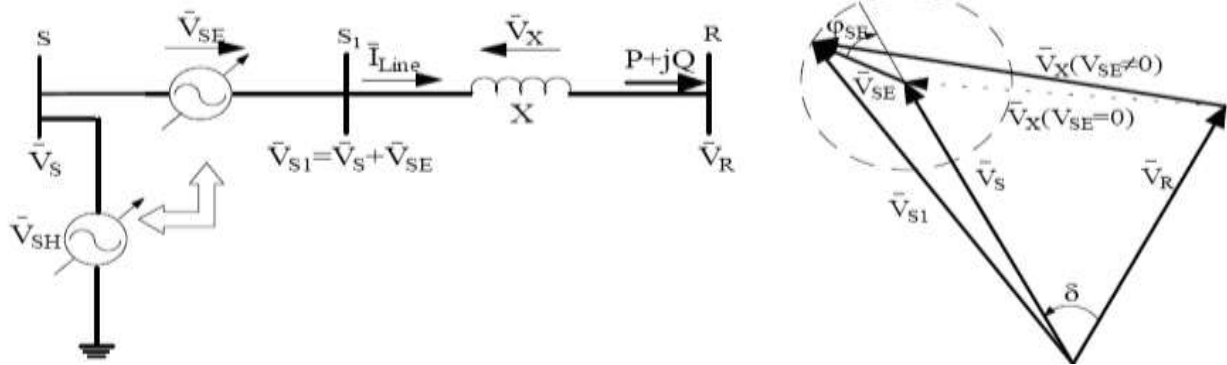


Fig. 5 Application of UPFC unit in the tie-line

UPFC is set in the transmission line between buses S and R as appeared in Fig 5. Line conductance was ignored. UPFC unit is represented by two ideal voltage sources of controllable magnitude and phase angle. In this case, the complex power received at the receiving end of the line is given by

$$S = \bar{V}_R \bar{I}_{Line}^* = \bar{V}_R \left(\frac{\bar{V}_S + \bar{V}_{SE} - \bar{V}_R}{jX} \right)^* \tag{7}$$

$$\bar{V}_{SE} = V_{SE} \angle (\delta_s - \varphi_{SE}) \tag{8}$$

The complex conjugate of this complex power is

$$S^* = P - jQ = \bar{V}_R^* \left(\frac{\bar{V}_S + \bar{V}_{SE} - \bar{V}_R}{jX} \right) \tag{9}$$

Performing simple measured manipulations and separating real and imaginary components of Eqn (9) the subsequent expressions for real and the reactive powers received at the receiving finale of the line are

$$P = \frac{V_S V_R}{X} \sin \delta + \frac{V_R V_{SE}}{X} \sin(\delta - \varphi_{SE}) = P_O(\delta) + P_{SE}(\delta, \varphi_{SE}) \quad (10)$$

$$Q = -\frac{V_R^2}{X} + \frac{V_S V_R}{X} \cos \delta + \frac{V_R V_{SE}}{X} \cos(\delta - \varphi_{SE}) = Q_O(\delta) + Q_{SE}(\delta, \varphi_{SE}) \quad (11)$$

The active and reactive power received at bus R for the system with the UPFC unit thus fitted can be controlled between the rotation of the sequentially injected voltage phasor with a value of V_{SEmax} from 0 to 360° allows the real and the reactive power flow to be controlled within the boundary

$$P_{\min}(\delta) \leq P \leq P_{\max}(\delta) \quad (12)$$

$$Q_{\min}(\delta) \leq Q \leq Q_{\max}(\delta) \quad (13)$$

From the physical perspective, it is noticed that the UPFC unit situated in the tie-line between two areas is effective to settle the inter-area oscillation mode just, and afterward, the HES unit is fit for providing the energy into the power system ought to be appropriate for the control of the inertia mode. The HES is demonstrated as an active power source to area-1 with the gain constant K_{HES} and time constant T_{HES} . The UPFC unit is displayed as a tie-line power flow controller with a time constant T_{UPFC} . The control gain of the HES unit and state feedback matrix K of UPFC unit are shown in appendix. In this study, a two-area interconnected thermal deregulated power system with HES and UPFC units model consisting of two thermal generating stations in each area is considered as shown in Fig 6. All generators are working with essential/ordinary programmed age control plan or accessibility based duty programmed based age control conspire and every generator is possessed by a different age organization. The execution of an accessibility based tax based programmed age control conspire is done for exchanging tasks between programmed age control and non-programmed age control mode, which depends on the distinction of the generator's minor expense and continuous recurrence subordinate cost of unscheduled age.

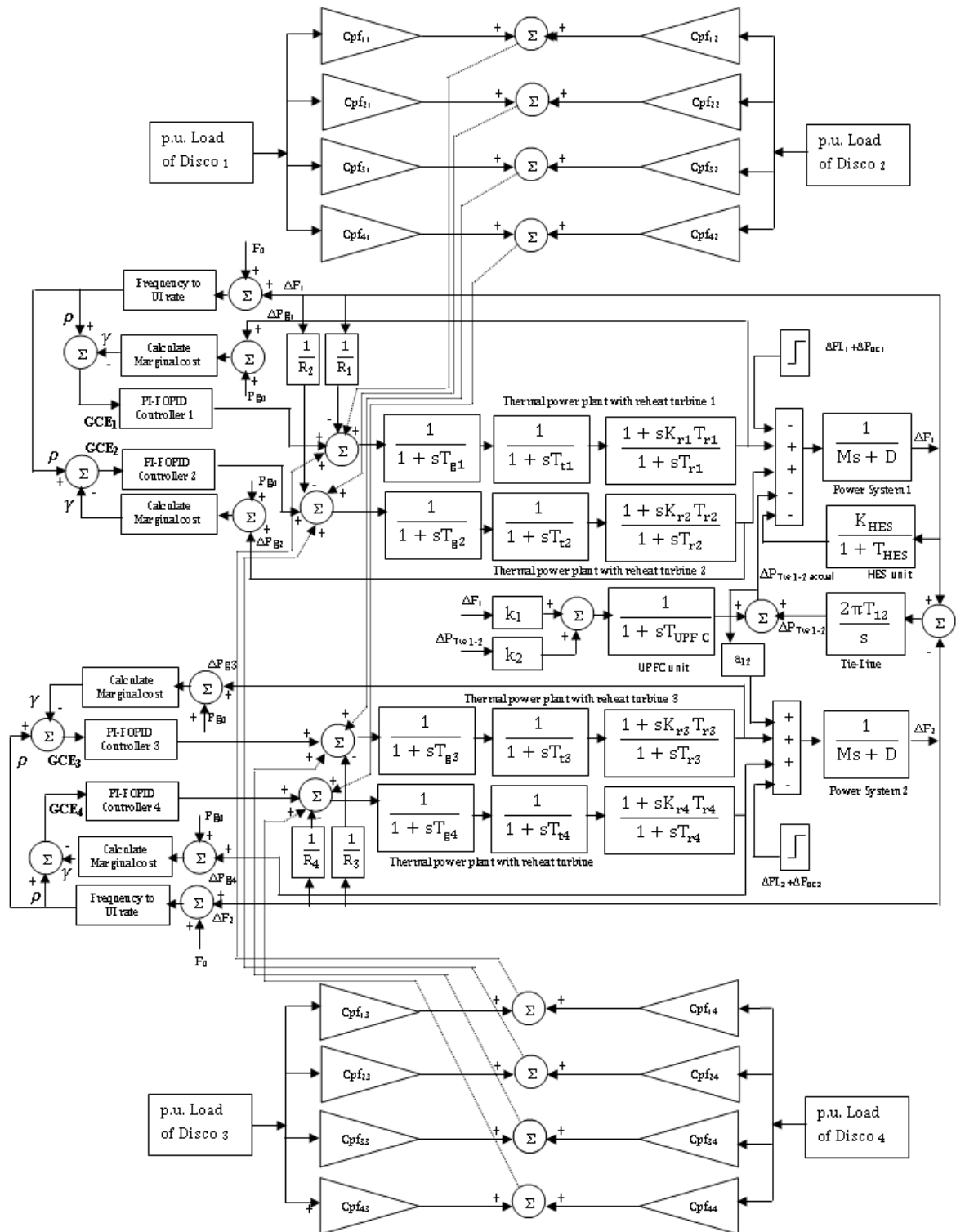


Fig. 6. Transfer function model of Price signal based Automatic Generation Control loop for a two area thermal-thermal deregulated power system with HES and UPFC units

4. Design Of PI-FOPID controllers using Moth-Flame Optimization (MFO) algorithm

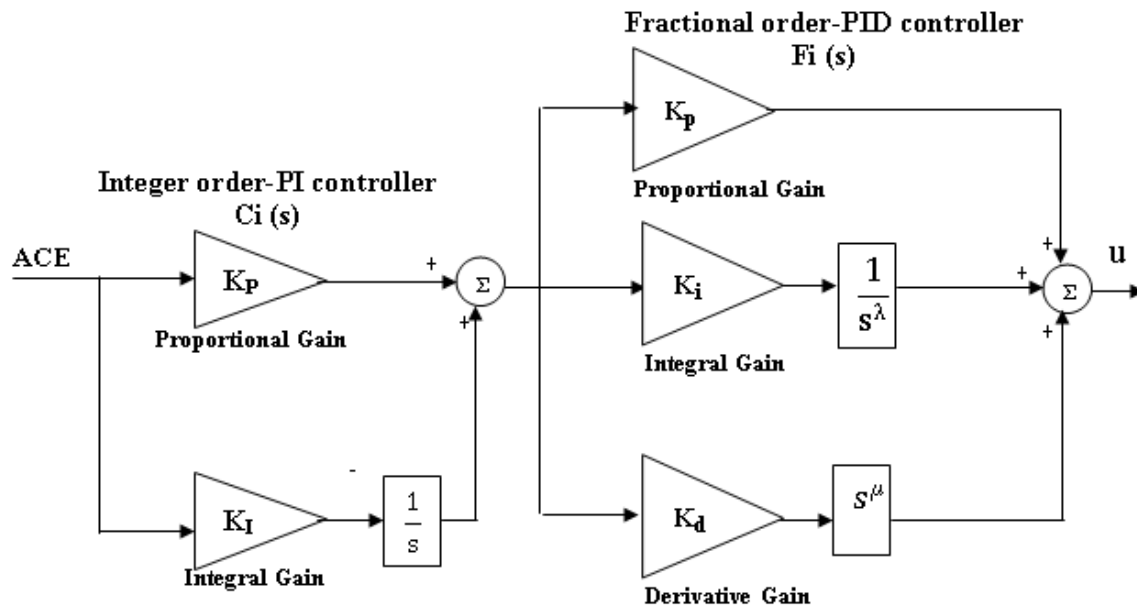


Fig. 7 Block diagram for IDN-FOPD controller

The cascade aggregate of Integer Order (IO) and Fractional Order (FO) controller's Proportional-Integral along with Fractional Order Proportional-Integral-Derivative (PI-FOPID) is recommended as a secondary controller for price based AGC loop of a two-area thermal deregulated power system. The detailed structure of PI-FOPID controller is pointed out in Fig 7. In this Figure, there are two blocks $C_i(s)$ and $F_i(s)$, where $C_i(s)$ and $F_i(s)$ represent the structure of the integer order- proportional-integral (PI) controller and fractional order- proportional-integral-derivative (FOPID) controller respectively.

The transfer function of the integer order-PI controller $C_i(s)$ is given by

$$C_i(s) = K_{Pi} + \frac{K_{Ii}}{s} \tag{14}$$

FOPID controller has μ as non-integer order of derivative that is a real number. Thus, transfer-function of FOPID controller $F_i(s)$ is given by

$$F_i(s) = K_{Pi} + \frac{K_{Ii}}{s^\lambda} + K_{di} s^\mu \quad \lambda, \mu > 0 \tag{15}$$

The overall transfer function of proposed PI-FOPID controller is given by

$$T_i(s) = (K_{Pi} + \frac{K_{Ii}}{s}) + (K_{Pi} + \frac{K_{Ii}}{s^{\lambda i}} + K_{di} s^{\mu i}) \quad (16)$$

The main function of AGC is to control load frequency and tie line power during load disturbance. So the GCE signals of frequency and tie line power are used as design criteria to tune the PI-FOPID controller. The error inputs to the controllers are the respective generation control errors (GCE) given by Eqn. (1). The control inputs of the power system with FOPID structure are given by

$$u_i = ((K_{Pi} GCE_i + K_{Ii} D^{-1i} GCE_i) + (K_{Pi} GCE_i + K_{Ii} D^{-\lambda i} GCE_i + K_{di} D^{\mu i} GCE_i) \quad (17)$$

In this study, Moth-Flame Optimization (MFO) algorithm is used to tune the PI-FOPID controller for a two area thermal-thermal interconnected power system. The performance of these responses is measured using performance functions such as Integral of Squared Error (ISE) given by Eqn (29).

$$J = \int_0^{t^{sim}} [(GCE_i)^2] dt \quad (18)$$

The problem constraints are the proposed controller parameter bounds. Therefore, the design problem can be formulated as,

$$\text{Minimize } J \quad (19)$$

Subject to

$$K_p^{min} \leq K_p \leq K_p^{max}, K_I^{min} \leq K_I \leq K_I^{max}, K_p^{min} \leq K_p \leq K_p^{max}, K_i^{min} \leq K_i \leq K_i^{max}, K_d^{min} \leq K_d \leq K_d^{max}, \lambda^{min} \leq \lambda \leq \lambda^{max}, \mu^{min} \leq \mu \leq \mu^{max} \quad (20)$$

4.2 Moth-flame optimization (MFO) Algorithm

Mirjalili proposed moth-flame optimization (MFO) in 2015 [10] that is motivated by the moths navigation approach. Moths rely upon transverse direction for route where a moth flies by possession up a settled point concerning the moon. Exactly when moths see the human-made fake light, they try to have a comparative point of the light to fly in the straight line. Moths and flares are the essential parts of the counterfeit MFO calculation. MFO is a

populace based calculation with the arrangement of n moths are utilized as search administrators. Blazes are the best N places of moths that are gained up until now. As such, every moth looks for around a fire and updates it if there ought to be an event of finding a superior arrangement. Given logarithmic winding, a moth refreshes its position concerning a given fire as in the Eqn (21) [8].

$$S(M_i, F_j) = D_i e^{bt} \cos(2\pi t) + F_j \quad (21)$$

where D_i shows the Euclidian distance of the i^{th} moth for the j^{th} flame, b is a constant to define the shape of the logarithmic spiral, M_i demonstrate the i^{th} moth, F_j shows the j^{th} flame, and t is a random number in $[-1, 1]$.

As might be found in the above equation, the next position of a moth is characterized with respect to a flame. The t boundary in the winding condition portrays how much the following situation of the moth should be close to the fire. The winding condition allows a moth to fly around a fire and not really in the space between flares considering both investigation and abuse of arrangements. With a particular ultimate objective to additionally underscore abuse, we guess that t is an irregular number in $[r, 1]$ where r is directly diminished from -1 to -2 through the range of accentuation and is called union consistent. With this method, moths will in general endeavor their comparing blazes all the more accurately relating to the quantity of cycles. So as to overhaul the probability of uniting to a worldwide arrangement, a given moth is obliged to refresh its position using one of the blazes (the relating fire). In each cycle and in the wake of refreshing the fire list, the blazes are arranged dependent on their wellness esteems. From that point forward, the moths update their situations with respect to their comparing blazes. To allow a lot of misuse of the best reassuring arrangements, the quantity of blazes to be taken after is lessened with respect to the cycle number as given in the Eqn (22).

$$N_{flames} = \text{round}\left(N - l * \left(\frac{N-1}{T}\right)\right) \quad (22)$$

where l is the present iteration number, N is the maximum number of flames, and T demonstrates the maximum number of iterations.

5. Simulation Results and Observations

In this test system consists of two Gencos and two Discos in each area. All the Gencos in every area consider as thermal reheat units. In this study, the PI-FOPID controllers are designed using Moth-flame optimization (MFO) algorithm and implemented in a two-area thermal-thermal reheat steam turbine power system with UPFC and HES units for various generation schedules as showed up in Fig 6. HES unit is introduced in area-1 and the SSSC unit is associated in series with the tie-line closer to area-1. The ideal arrangement of control inputs is taken for improvement issue and the target work in Eqn (18) is determined to utilize the Generation Control Error (1).

Under current regulations (CERC, 2009), UI price is pegged at 1800 ₹/MWh at 50 Hz frequency. This means that if one and all (Generators and Loads) adhere to the plan, the frequency ought be 50 Hz and UI price 1800 ₹/MWh. However, at 1800 ₹/MWh UI price some generators get an error signal causing them to deviate from their schedule. This may even cause the frequency to depart from nominal value. This outcome is undesirable, as it results in UI among generators even when load is as per schedule. To illustrate our point, we simulated an isolated area system having a capacity of 3000 MW supplied by two generating stations. The relevant data shown in appendix. The system data is given in Table 1. The generator capacities and their cost coefficients are given in Table 2. The power generations are given in Table 3 for various schedules and their corresponding marginal costs are given in Table4. Here every one of the Discos has the contract with the Gencos and the accompanying Disco Participation Matrix (DPM) alluding to Eq (23) is considered as

$$DPM = \begin{bmatrix} 0.2 & 0.3 & 0.1 & 0.4 \\ 0.3 & 0.2 & 0.3 & 0.1 \\ 0.25 & 0.1 & 0.25 & 0.3 \\ 0.25 & 0.4 & 0.35 & 0.2 \end{bmatrix} \quad (23)$$

Case 1: The generators are scheduled in merit order and load level results in system marginal cost of 1800 ₹/MWh. This situation characterizes the only case in which price based AGC works successfully. The scheduled generation of this scenario is given in first row of Table 3. For this scenario, the generation is scheduled so that the overall system marginal cost is 1800 ₹/MWh. The load level does not change during the simulation. This means that none of the generators will get any error signal. The outcome of simulation is shown in Fig 8. It is observed that there is no impact on either frequency/UI price or scheduled generation. Investigation reveals on comparison of dynamic responses the proposed PI-FOPID controller in all transaction policies explores the dominance of the concluding in terms of peak deviations, settling time and scale of oscillations as compared to the FOPID controller. The significant advantage of PI-FOPID controllers is flexibility in controlling purpose which helps to design the AGC problems and excellent capability of handling parameter uncertainty, elimination of steady state error and better stability. It is also inferred that use of HES and UPFC units improve the system performance in terms of reduces peak deviations, settling time and magnitude of oscillations.

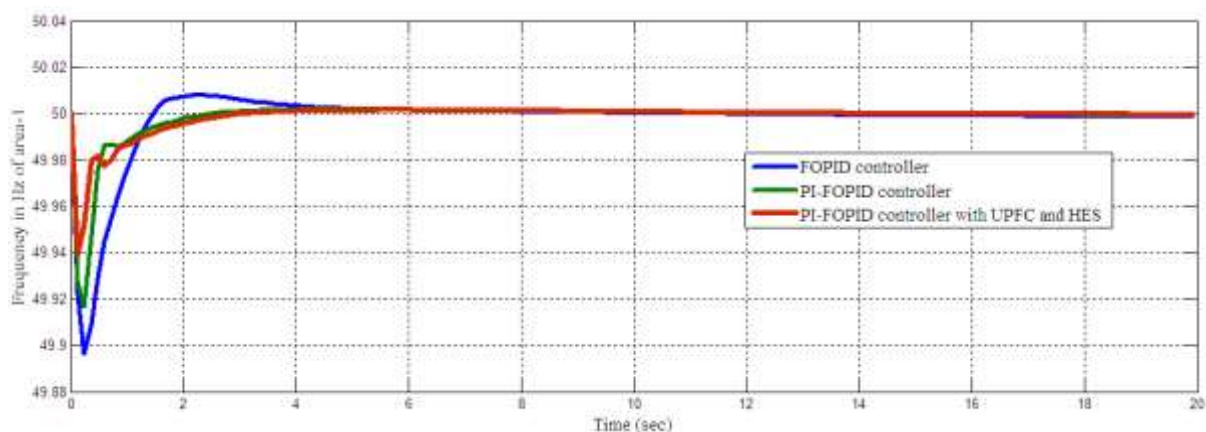


Fig. 8(a) Frequency in Hz of Area-1

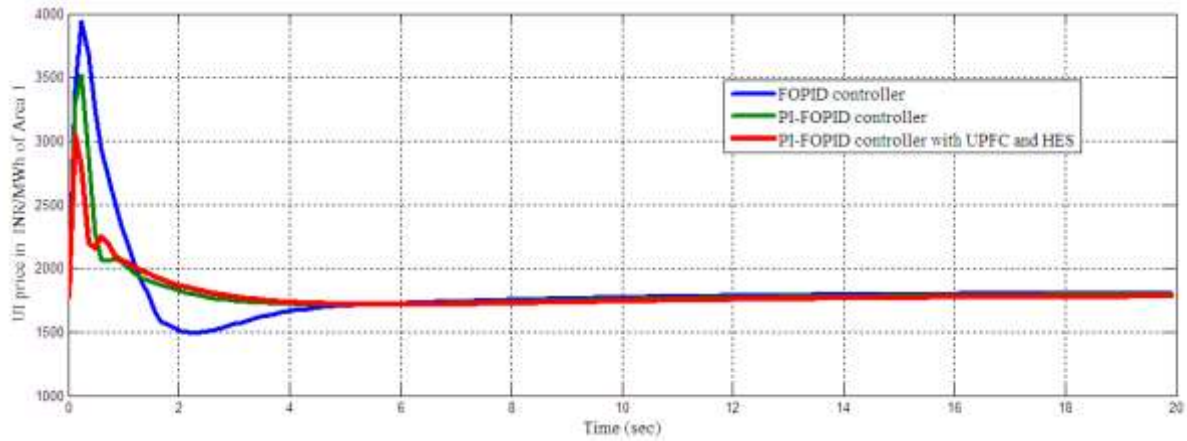


Fig. 8(b) UI price in ₹/MWh of Area-1

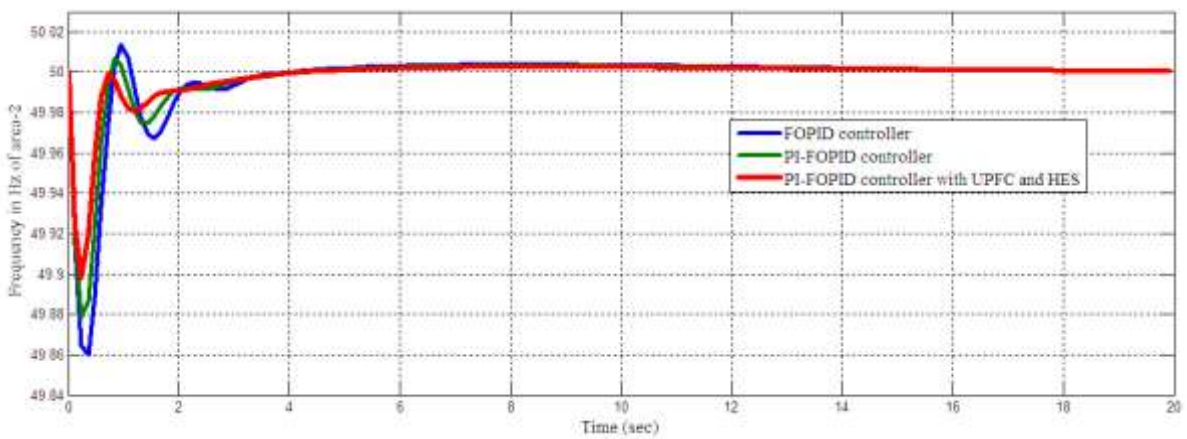


Fig. 8(c) Frequency in Hz of Area-2

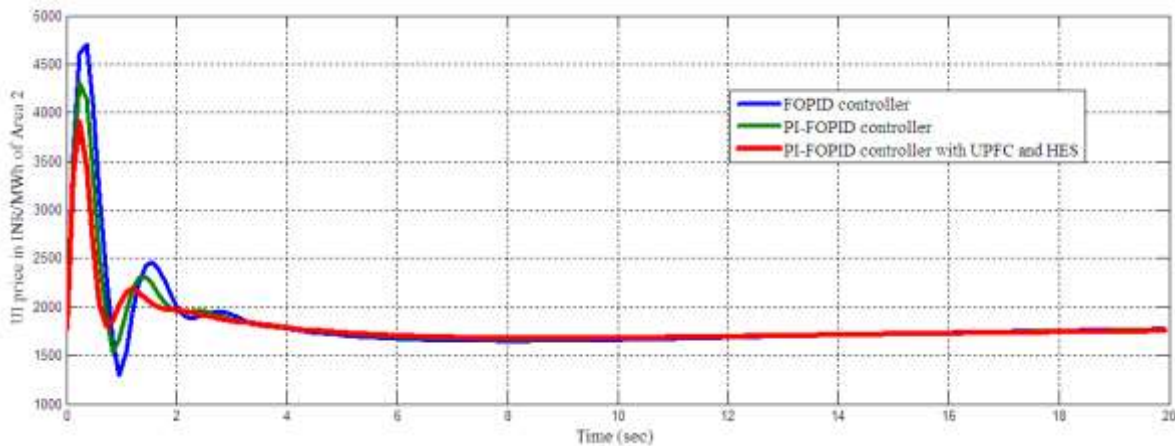


Fig. 8(d) UI price in ₹/MWh of Area-2

Case 2: The generators are scheduled in merit order and the system marginal cost is equal to the reference UI price of CERC 2009 regulations. A load increase of 400 MW in area 1 is considered. The power generations of schedule 1 from Table 3 is considered. As the load is increased by 400 MW, the total load on the system becomes 3483.33 MW. Allocating this

total load on equal marginal cost basis Genco₁ and Genco₂ in area 1 will get additional 200 MW each. With this new generation schedule, the system frequency response and UI price and change in generation power is shown in Fig 9. As the system frequency in area 1 deviated its nominal value with the sudden increase in load, it has to pay the UI charge is 2000 ₹/MWh and with use HES and UPFC units to pay the UI charge is reduced by 1770 ₹/MWh. Investigation reveals on comparison of dynamic responses the proposed PI-FOPID controller explores the superiority of the latter in terms of peak deviations, settling time and magnitude of oscillations as compared to the FOPID controller. It is also inferred that use of HES and UPFC units recover the system presentation in terms of reduces peak deviations, settling time and magnitude of oscillations.

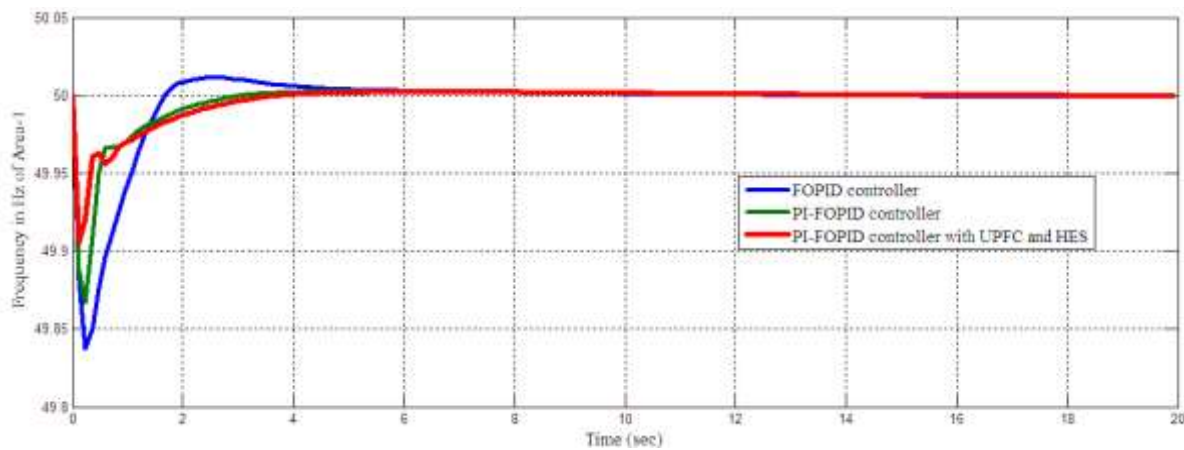


Fig. 9(a) Frequency in Hz of Area-1

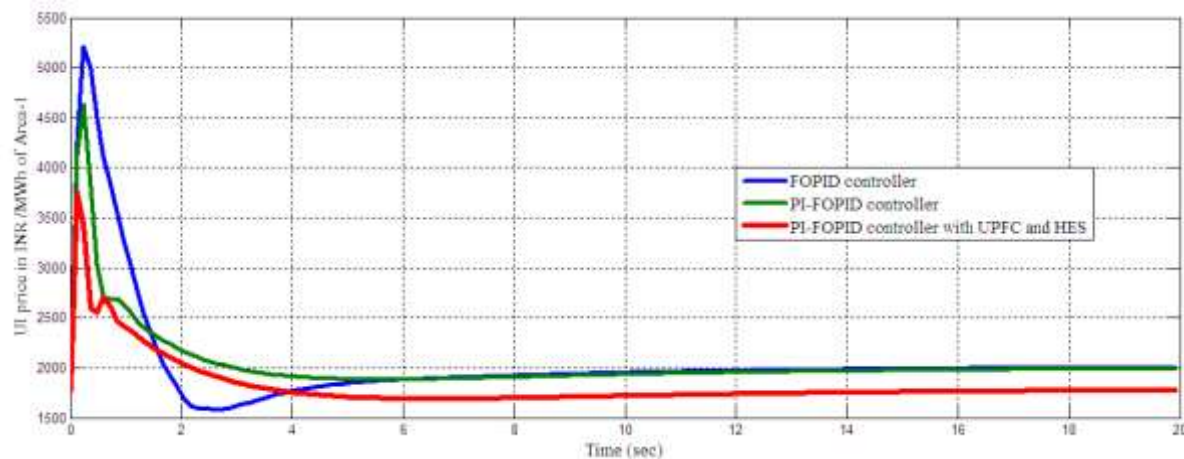


Fig. 9(b) UI price in ₹/ MWh of Area-1

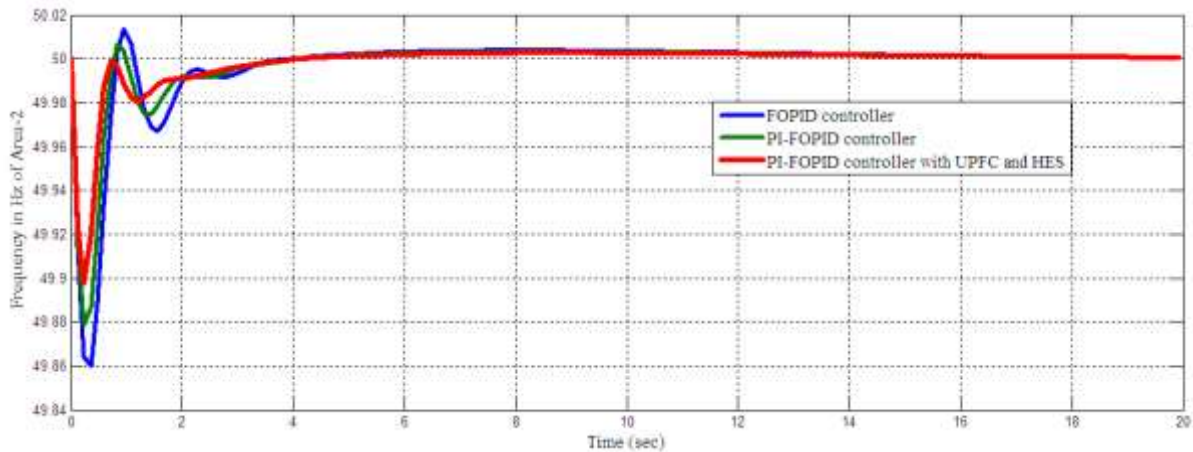


Fig. 9(c) Frequency in Hz of Area-2

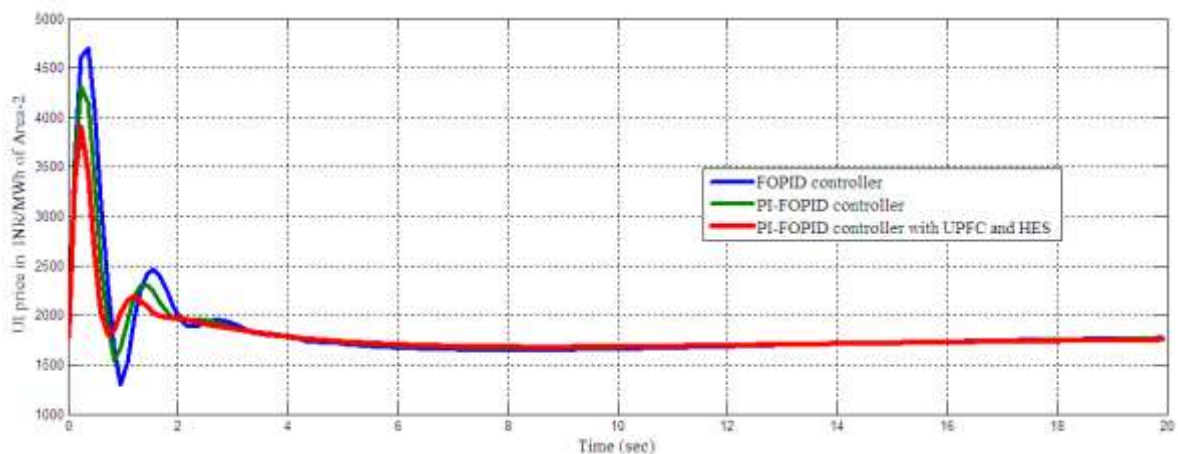


Fig. 9(d) UI price in ₹/MWh of Area-2

Case 3: The generators are scheduled in merit order and the system marginal cost is equal to the reference UI price. A load is decrease of 200 MW in area 1 is considered. The power generations of schedule 1 from Table 3 is considered. As the load is decrease by 200 MW, the total load on the system becomes 2883.33 MW. Allocating this total load on equal marginal cost basis Genco₁ and Genco₂ in area 1 will get reduced power generation of 100 MW each. With this new generation schedule, the system frequency response and UI price and change in generation power is shown in Fig 10. As the system frequency in area-1 more than the nominal value with the sudden decrease in load, it has to pay the UI charge is reduced 1600 ₹/MWh from the nominal price 1800 ₹/MWh at 50 Hz. A growth in frequency is observed and therefore the UI price falls to around 1600 ₹/MWh. Only Generators 1 and 2

are proficient of reducing their outputs. A growth in frequency is observed and accordingly the UI price falls to around 1400 ₹/MWh with use of HES and UPFC units. Moreover HES unit having loading capacity in accumulating to the kinetic energy of the generator rotors is prudent to reduced the peak frequency oscillations of both areas. UPFC device can be installed in arrangement with the tie-line between any interconnected zones to settle the zone recurrence motions by rapid control of tie-line power through the interconnections. Moreover, the critical observation shows that the proposed PI-FOPID controller having more tuning parameters performs much better than the FOPID controller having the less peak deviations, settling time and magnitude of oscillations of the dynamic output response.

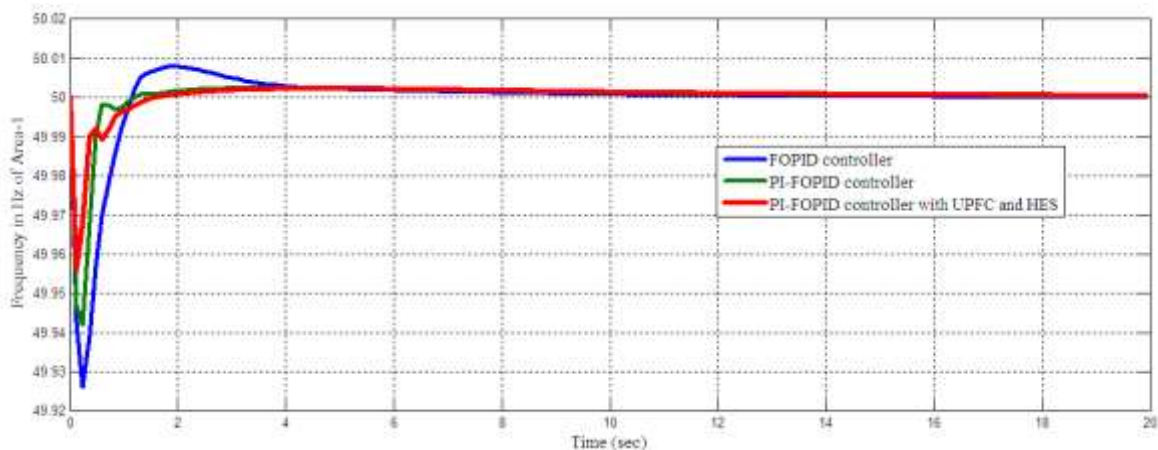


Fig. 10(a) Frequency in Hz of Area-1

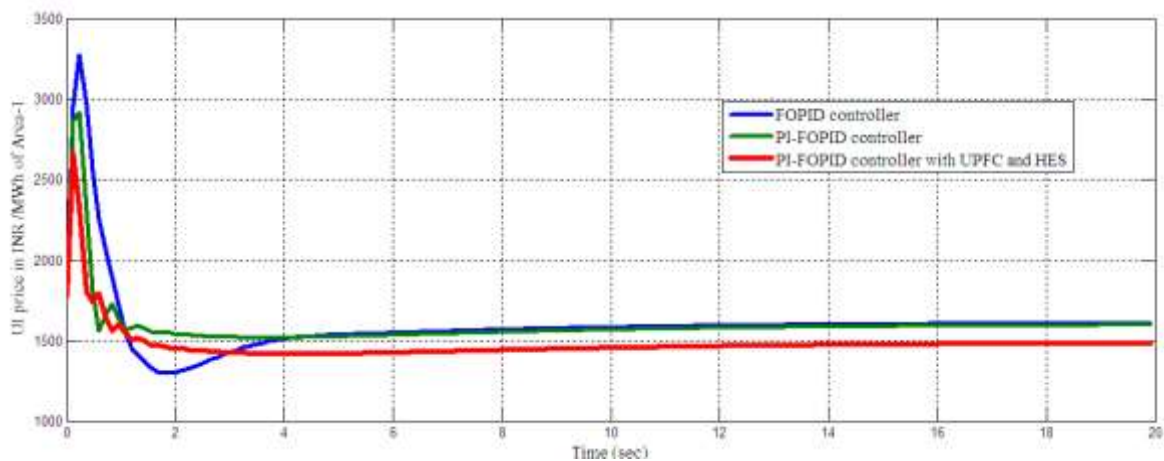


Fig. 10(b) UI price in ₹/MWh of Area-1

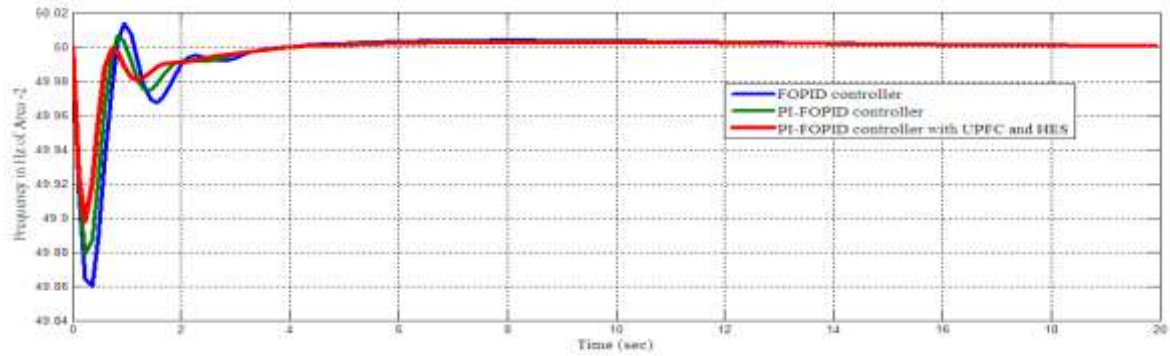


Fig. 10(c) Frequency in Hz of Area 2

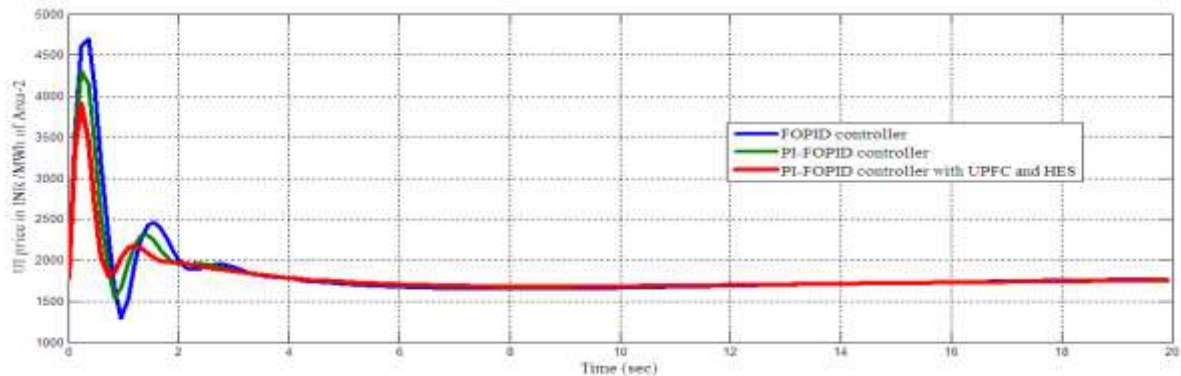


Fig. 7(d) UI price in ₹/MWh of Area 2

Conclusion

The PI-FOPID controllers are designed using MFO algorithm technique and implemented for price based AGC loop of a two-area thermal interconnected power system without and with HES and UPFC units for different case studies. A new scheme is presented to generate power based on GCE using the UI prices and the marginal costs to minimize the UI charge by mitigating the frequency deviations and to maintain the desired generation schedule. Frequency stability and economic operation are simultaneously achieved through this scheme and no tertiary control loop is required for this purpose as in the instance of ordinary AGC. Execution of proposed control on all focal and state producing stations won't just outcomes in a superior control of recurrence, yet additionally guarantees the legitimacy request dispatch of age simultaneously.. Investigation reveals on contrast of dynamic responses the proposed based PI-FOPID controller in all case studies explores the dominance of the latter in terms of peak deviations, settling time and scale of

oscillations as compared to the FOPID controller. The significant advantage of PI-FOPID controllers is flexibility in controlling purpose which helps to design the AGC problems and excellent capability of handling parameter uncertainty, elimination of steady state error and better stability. Moreover, HES and UPFC units have been coordinated with the price based AGC loop for a two-area thermal interconnected deregulated power system not only improves the power system dynamics but also reduces the UI price.

Acknowledgement

The authors wish to thank the authorities of Annamalai University, Annamalainagar, Tamilnadu, India for the facilities provided to prepare this paper.

References

- [1] Fosha, C.E. and Elgerd, O.I., (1970), The Megawatt Frequency Control problem: A New Approach via Optimal Control Theory, *IEEE Transactions on Power Apparatus and Systems*, Vol. PAS-89 (4), pp. 563-574.
- [2] Pappachen, A. and Fathima, A.P., (2017), Critical research areas on load frequency control issues in a deregulated power system: A state-of-the-art-of-review, *Renewable and Sustainable Energy Reviews*, Vol.72, pp.163-177.
- [3] Pujara, S. M., and Kotwal, C. D., (2016), An inclusive review on load frequency control in deregulated market, *International Journal on Electrical Engineering and Informatics*, Vol.8(3), pp.595-611.
- [4] Hasan, N., Ibraheem, and Ahmad, S., (2016), ABT based load frequency control of interconnected power system, *Electric Power Components and Systems*, Vol.44(8), pp.853-863.
- [5] Saikia, L.C., Nanda, J. and Mishra, S., (2011), Performance comparison of several classical controllers in AGC for multi-area interconnected thermal system, *International Journal of Electrical Power & Energy Systems*, Vol.33(3), pp.394-401.
- [6] Sahu, R. K., Panda, S., and Padhan, S., (2014), Optimal gravitational search algorithm for automatic generation control of interconnected power systems, *Ain Shams Engineering Journal*, Vol.5 (3), 721-733.
- [7] Sahu, R. K., Panda, S., Biswal, A., and Sekhar, G. C., (2016), Design and analysis of tilt integral derivative controller with filter for load frequency control of multi-area interconnected power systems, *ISA transactions*, Vol.61, pp.251-264.
- [8] Kumar, N., Tyagi, B., and Kumar, V., (2018). Application of fractional order PID controller for AGC under deregulated environment, *International Journal of Automation and Computing*, Vol.15 (1), pp.84-93.
- [9] Saha, D., and Saikia, L. C., (2017), Performance of FACTS and energy storage devices in a multi area wind-hydro-thermal system employed with SFS optimized I-PDF controller, *Journal of Renewable and Sustainable Energy*, Vol.9(2), pp.024103.
- [10] Mirjalili, S., (2015), Moth-flame optimization algorithm: A novel nature-inspired heuristic paradigm, *Knowledge-based systems*, Vol.89, pp.228-249.

[11] Shankar, R., Chatterjee, K and Bhushan, R., (2016), Impact of energy storage system on load frequency control for diverse sources of interconnected power system in deregulated power environment, *International Journal of Electrical Power & Energy Systems*, Vol.79, pp.11-26.

[12] Baskar, B., Paramasivam, B., and Chidambaram, I. A.,(2018),Ancillary Service Requirement based Automatic Generation Control Assessment in a deregulated power system with HES and IPFC units, *Journal of Engineering Science and Technology*, Vol.13(10), pp.3092-3115.

[13] G. Ganesan @ Subramanian, I.A. Chidambaram and J. Samuel Manoharan (2019), “Pseudo-Derivative Feedback controller for Automatic generation control in a deregulated power system with Hydrogen-Energy storage”, *Caribbean Journal of Science*, vol.53, issue:1 (Jan-Apr), pp: 56-79.

[14] Parvathy, S., and Thampatty, K. S., (2015). Dynamic modeling and control of UPFC for power flow control, *Procedia Technology*, Vol.21, pp.581-588.

APPENDIX

Table 1 System data [4, 5]

Capacity = 3000 MW
M= 1000 MW-s/Hz
D= 100 MW/Hz
F ⁰ =50 Hz
R ₁ = R ₂ = R ₃ = R ₄ = 2.4 Hz / p.u.MW
T _{g1} = T _{g2} = T _{g3} = T _{g4} = 0.08 s,
T _{r1} = T _{r2} = T _{r1} = T _{r2} = 10 s
T _{t1} = T _{t2} = T _{t3} = T _{t4} = 0.3 s
K _{r1} = K _{r2} = K _{r3} = K _{r4} = 0.5
2πf ₁₂ = 0.545 p.u.MW / Hz, a ₁₂ = -1

Table 2 Generator Data [4, 5]

	Genco ₁	Genco ₂	Genco ₃	Genco ₄	
Capacity (MW)	1500	1500	1500	1500	
Cost Coefficients	bi (₹/MWh)	800	1000	800	1000
	ci (₹/MW ² h)	0.3	0.3	0.3	0.3

Table 3 Generation Schedule (in MW) [4, 5]

	Genco ₁	Genco ₂	Genco ₃	Genco ₄
Schedule 1	1500	1333.33	1500	1333.33
Schedule 2	1500	1500	1500	1500
Schedule 3	1500	1500	1500	1500

Table 4 Marginal Costs in ₹/MWh [4, 5]

	Genco ₁	Genco ₂	Genco ₃	Genco ₄
Schedule 1	1700	1800	1800	2000
Schedule 2	1700	1700	1700	2000
Schedule 3	1700	1900	1900	2000

Table 1d: Data for the HES and SSSC unit [9,10]

Parameter	K_{AE}	T_{AE} (sec)	K_{FC}	T_{FC} (sec)	T_{UPFC} (sec)	k_1	k_2
Value	0.002	0.5	0.01	4	0.15	0.45	0.52